Asymmetric $(e,2e)$ study of the 100-eV ionization of the $3\sigma_g$ and $1\pi_u$ molecular orbitals of N_2

J. P. Doering and J. Yang
Department of Chemistry, Johns Hopkins University, Baltimore, Maryland 21218-2685
(Received 18 January 1996)

Electron-impact ionization of the $3\sigma_g$ and $1\pi_u$ molecular orbitals of N_2 to produce the $X\,^2\Sigma_g^+$ and $A\,^2\Pi_u$ states of N_2^+ has been investigated in an asymmetric $(e,2e)$ experiment at the 100-eV maximum of the total ionization cross section. The experiment allows the direct comparison of ionization of two molecular orbitals in the same target molecule. Scattering angles of the incident electron $<5°$ and ejected electron energies from 3 to 13 eV were used. The relative triple differential cross sections were obtained as a function of ejected electron angle for both the binary (parallel to momentum transfer direction) and recoil (antiparallel) directions. The maxima of the binary and recoil peaks were found to be shifted from the angular positions predicted by first-order theory. In contrast to the typical atomic case, the recoil peaks were shifted to smaller ejection angles. In addition, the binary peak of the $1\pi_u$ orbital ionization was located at an angle 30° larger than the corresponding peak for the $3\sigma_g$ orbital. These results suggest that the experiment is very sensitive to the initial and final states of the target. Differences from results with atomic targets may be related to the nonspherically symmetric nature of the target and residual ion. [S1050-2947(96)06209-9]

PACS number(s): 33.80.−b

INTRODUCTION

$(e,2e)$ or electron-electron coincidence ionization experiments provide a very sensitive method for the study of ionization processes [1,2]. In such experiments, the energy and momentum of the incident electron before and after the collision with the target, the energy and momentum of the ejected or secondary electron, and the final electronic state of the residual ion are all determined. Although there is now extensive $(e,2e)$ data on atoms, most experiments on molecules so far have been performed either in the binary regime to measure momentum distributions of electrons in various orbitals [3] or in the dipole regime, which simulates photoionization conditions [4]. Only a few molecular $(e,2e)$ experiments have been carried out under conditions typical of the majority of ionization events: momentum transfer values between 0.2 and 1.0 a.u. and unequal sharing of energy between the two outgoing electrons so that the ejected or secondary electron has much less energy than the scattered incident electron [1].

Experiments with unequal sharing of the excess energy between the two outgoing electrons are known as asymmetric $(e,2e)$ experiments. As in all $(e,2e)$ experiments, they can be characterized by a triple differential ionization cross section (TDCS). For a fixed incident energy, E_0, the TDCS is

$$d^3\sigma/dE_{\rm ej}d\Omega_0 d\Omega_{\rm ej}. \tag{1}$$

$E_{\rm ej}$ is the energy of the ejected electron, Ω_0 is the solid angle into which the incident electron is scattered, and $\Omega_{\rm ej}$ is the solid angle into which the low-energy secondary electron is ejected. Although there are two energy variables, E_0' and $E_{\rm ej}$, where E_0' is the energy of the incident electron after the collision, only one energy is an independent variable when the final state of the ion is known from the measured energy parameters of the experiment. Experiments are usually carried out for the case in which the momentum vectors of the incident, scattered, and ejected electrons are coplanar. Under these conditions, Ω_0 and $\Omega_{\rm ej}$ can be replaced by the in-plane angles θ_0 and $\theta_{\rm ej}$ and (1) becomes

$$d^3\sigma/dE_{\rm ej}d\theta_0 d\theta_{\rm ej}. \tag{2}$$

When displayed as a function of $\theta_{\rm ej}$ at a fixed θ_0 and $E_{\rm ej}$, asymmetric $(e,2e)$ triple differential cross sections are characterized by two maxima [1]. The positions of the maxima are related to the direction of momentum transfer in the ionizing collision. The momentum transferred to the target is

$$\mathbf{K}=\mathbf{k}_0-\mathbf{k}_0', \tag{3}$$

where $\mathbf{k}_0$ and $\mathbf{k}_0'$ are the initial and final momenta of the incident electron. The maximum in the direction of the momentum transfer is known as the ''binary peak'' while the maximum in the opposite direction, which arises from interaction of the ejected electron with the ion core, is known as the ''recoil peak.'' For high incident energy and very small momentum transfer the ionization is well described by the first Born approximation [1]. First-order theory requires that the binary and recoil peaks lie on a common axis oriented to coincide with the direction of the momentum transfer vector. At low to medium K values ($0.2<K<1.0$ a.u.) and for low values of E_0, deviations from the predictions of the first Born approximation are observed [1]. For atoms, both the binary and recoil peaks are characteristically displaced to larger angles than the direction of the momentum transfer vector so that the maxima of the binary and recoil peaks no longer lie on a common axis. This deviation from first-order behavior is apparently a very sensitive function of the interactions between the residual ion core and the two outgoing electrons [1].

One goal of the present experiments on N_2 is to determine whether such deviations appear in a typical molecular case and if so, to determine their extract form. As the residual molecular ion is not generally spherically symmetric,

the interactions of the two outgoing electrons can be expected to be more complicated than for the atomic case.

Only a few asymmetric $(e,2e)$ experiments on valence orbitals of molecules have been performed in the low incident energy, intermediate momentum transfer region. Extensive measurements of the absolute triple differential cross section are available only for H_2 [5]. Limited data are available for the N_2 $3\sigma_g$ orbital and the carbon $\sigma 1s$ molecular orbital of acetylene [6–8]. In their N_2 work, Jung *et al.* [6] used an incident energy of 100 eV, incident electron scattering angles from 8° to 25°, and ejected electron energies of 3 and 4 eV, whereas Avaldi *et al.* [7] used an incident energy of 270 eV, incident electron scattering angles from 3° to 8°, and ejected electron energies of 10 and 18.8 eV. Jung *et al.* [6] found that in most cases the recoil peak was absent or very weak while Avaldi *et al.* [7] found a binary-recoil peak ratio near unity. For the carbon $\sigma 1s$ orbital of acetylene, Avaldi *et al.* [8] found that the recoil peak was displaced to smaller angles than first-order theory would predict, in contrast to typical atomic results.

In the present work, we have investigated the 100-eV TDCS for production of the $X\,^2\Sigma_g^+$ and $A\,^2\Pi_u$ states of N_2^+ produced by removal of an electron from the $3\sigma_g$ and $1\pi_u$ molecular orbitals of N_2. N_2 is a particularly interesting target molecule because of the importance of N_2 ionization processes in planetary atmospheres. An incident energy of 100 eV was chosen because this incident energy is almost exactly the energy of the maximum of the N_2 total ionization cross section $[\sigma(E_0)]$ [9]. The TDCS has been investigated for small scattered electron angles ($<5°$) and ejected electron energies from 3 to 10.5 eV. Results from two previous experiments carried out with an older version of the apparatus have already been published [10,11]. In the first, the TDCS was measured at a fixed ejected electron angle of 74°. In the second, a limited measurement was made of the angular distribution ejected electrons. The present experiments include much more extensive TDCS measurements with an improved apparatus.

APPARATUS

Earlier versions of the apparatus have been described previously [10,11] so only a brief description will be given here with emphasis on new features. A schematic diagram of the apparatus is shown in Fig. 1. The electron monochromator, which produces the incident beam, and the scattered electron analyzer have essentially the same electron-optical design as the electron spectrometer described by Doering *et al.* [12] although a new construction method was used for the monochromator [13]. The use of an electron monochromator for the incident beam allowed experiments to be performed at better energy resolution than the typical energy spread of an electron beam from a hot-filament electron gun source [$\sim$0.6-eV full width at half maximum (FWHM)]. Data have been obtained with energy resolution as high as 0.19 eV although the typical resolution used for the present work was 0.35–0.40 eV. The third, ejected electron, analyzer, used to analyze the low-energy (3–13 eV) ejected electrons, was a 2.54-cm radius-of-curvature hemispherical analyzer preceded by a collimator and a three-element lens system.

The entire spectrometer was housed in a stainless steel

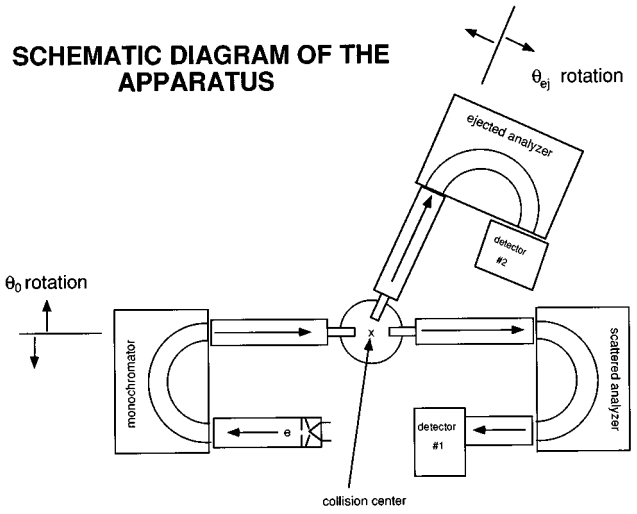

FIG. 1. Schematic diagram of the apparatus. The ejected analyzer's angle of rotation with respect to the incident beam direction is θ_{ej}. Rotation of the monochromator by changing θ_0 switches from binary to recoil scattering. The scattered electron analyzer is fixed.

bell jar approximately 0.5 m in diameter and 1 m high. The bell jar was surrounded by a double magnetic shield, which reduced the magnetic field at the spectrometer's position to <5 mg. The apparatus was differentially pumped with two 400-l/s turbopumps. One pump evacuated the volume around the spectrometer while the other provided differential pumping by evacuating the source region. Target gas densities at the collision center of the order of 10^{14} cm^{-3} were used. It was not possible to measure the pressure at the orifice of the hypodermic needle source directly. The density of target gas at the collision center was estimated from the pressure in the inlet system outside the vacuum system and the pressure inside the bell jar. An important improvement over previous versions of the apparatus [10,11] was the incorporation of an angle drive on the electron monochromator as well as on the ejected electron analyzer. This allowed both the scattered and ejected electron angles (θ_0 and θ_{ej} in Fig. 1) to be changed without opening the vacuum system and greatly increased the accuracy of the binary-recoil peak intensity ratio measurements.

The beam-steering deflectors in the spectrometer were adjusted to give equal inelastic scattering intensity from the intense 12.98-eV peak in the N_2 inelastic scattering spectrum on either side of $\theta_0=0$. This ensured that the spectrometer was adjusted properly when the monochromator was rotated to switch between the binary and recoil lobes.

The apparatus was operated at low angular resolution to improve the data rate. The primary electron beam's angular divergence was measured by the scattered electron analyzer. The beam was normally 4° wide (FWHM). The angle of the momentum transfer vector θ_K is given by

$$\sin\theta_K=(k_0'\sin\theta_0)/K. \tag{4}$$

[Note that in the coordinates used to display the TDCS, [1] the scattered incident electron is conventionally directed to a positive angle and the momentum transfer vector is therefore

directed to a negative angle. For simplicity, we calculate $|\theta_K|$ in (4).] At a scattering angle of $4°\pm2°$, 100-eV incident energy, and 10-eV ejected electron energy, the $\pm2°$ uncertainty in θ_0 causes an uncertainty of approximately $\pm10°$ in θ_K. This angular width is still much smaller than the typical measured $60°-70°$ angular width of the binary peak of the TDCS. The angular width of the ejected electron analyzer was investigated using the SIMION [14] ray-tracing program and found to be approximately 4°—much less than the uncertainty in θ_K.

Standard electronics as described previously [10] were used. Pulses from the two electron multiplier detectors were amplified, passed through a discriminator, and applied to the ''start'' and ''stop'' inputs of a time-to-amplitude converter (TAC). The output of the TAC was sent to a pulse height analyzer that produced and displayed a ''time spectrum.'' The time spectrum consisted of a time-correlated coincidence peak superimposed on a background of accidental coincidences.

For operation in the ''spectrum'' mode described below, a window discriminator was set to include only the time region containing the coincidence peak superimposed on the accidental background. The output of this discriminator was sent to a second computer, which recorded the coincidence plus background rate as a function of energy loss of the incident electron as the spectrum was scanned repeatedly.

There are two modes of operation of the apparatus. In the first ''spectrum'' mode, the energy loss of the incident electron is varied by scanning E_0' while keeping E_0 constant. The ejected electron analyzer is adjusted to detect ejected electrons at a fixed energy, $E_{\rm ej}$. A ''coincidence energy-loss'' spectrum is produced since by conservation of energy,

$$\Delta E = E_0 - E_0' = E_{\rm ej} + V_{\rm ion}(i), \tag{5}$$

where ΔE is the energy loss of the primary electron. When the energy loss is equal to the sum of the ejected electron energy and one of the ionization potentials of the target, a coincidence signal is produced. At other values of energy loss, no coincidence signal is produced.

A coincidence energy-loss spectrum is similar to a separation spectrum [7]. However, in a separation spectrum, the energy loss is fixed and the ejected electron energy is scanned. At high incident energy and small momentum transfer, this method of operation produces a spectrum closely related to a photoionization spectrum since the energy loss of the incident electron is equivalent to the photon energy. We operated the spectrometer at constant ejected energy with a variable energy loss of the scattered electron to avoid spectrometer transmission effects. The scattered electron analyzer was known to have constant transmission as a function of energy loss, but, because of the low electron energy and simple lens system, the transmission of the low-energy ejected electron analyzer was not constant as a function of ejected electron energy.

A typical coincidence energy-loss spectrum is shown in Fig. 2. This 200-point spectrum was taken at $E_{\rm ej}=3$ eV, $\theta_{\rm ej}=-72°$, $\theta_0=4°$. The raw data have been smoothed with a three-point running average program. The actual number of counts in each channel is shown for the approximately 1300-sec accumulation time per channel. The three peaks in the

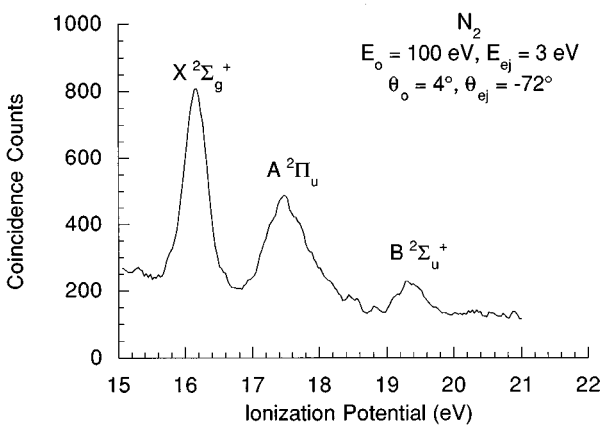

FIG. 2. 200-point coincidence energy-loss spectrum of N_2 at 100-eV incident electron energy for the ejected electron energy and angle, and incident electron scattering angle shown. The electronic states of N_2^+ associated with each of the three peaks are shown. The incident electron current was 1.6 nA and the total accumulation time was 1300 sec/channel.

spectrum correspond to production of the $X\,^2\Sigma_g^+$, $A\,^2\Pi_u$, and $B^2\Sigma_u^+$ electronic states of N_2^+ at ionization potentials of 15.57, 16.68, and 18.73 eV, respectively. The spectrum is superimposed on a background of accidental coincidences.

A close examination of Fig. 2 shows that the peaks do not appear at the exact spectroscopic values of the ionization potentials. The peak of the $X\,^2\Sigma_g^+$ state of N_2^+ appears at an energy loss of 16.16 eV rather than 15.57 eV. This discrepancy is the result of the contact potential in the electron source. The offset of the peaks arises in the following way. The zero of energy loss was established by making zero energy loss coincide with the maximum intensity of the elastically scattered beam. Since the scattered electron analyzer measures only the energy loss defined in (3), the contact potential in the source canceled. However, the ejected electron energy was set by adjusting the electron source voltage to a nominal value (2.5 eV for the spectrum in Fig. 2, for example) and tuning the analyzer to transmit electrons of this energy. The voltage applied to the electron source is referenced to ground potential as is the deflection voltage of the ejected electron analyzer. The actual energy of the electrons emerging from the source that the ejected electron analyzer is tuned to pass is therefore the sum of the applied voltage and the contact potential. Thus for the spectrum in Fig. 2, the contact potential was -0.59 V and the actual energy of the ejected electron was 3.09 eV. The contact potential varied between -0.45 and -0.85 V during these experiments. For convenience, the ejected electron energies are reported here rounded to the nearest 0.5 eV, uncertain by ±0.25 eV.

In the second, ''ejected angle scane,'' mode of operation, the ejected electron angle is varied while the other energies and angles are held fixed. A coincidence energy-loss spectrum is first obtained to locate the maximum of the ionization process to be studied. Then, as the ejected electron angle is varied, the apparatus is alternately tuned to the energy loss of the maximum and to a background energy loss where no coincidence signal is present. The coincidence rate is obtained by subtracting the background count rate from the coincidence plus background rate. A coincidence rate for a

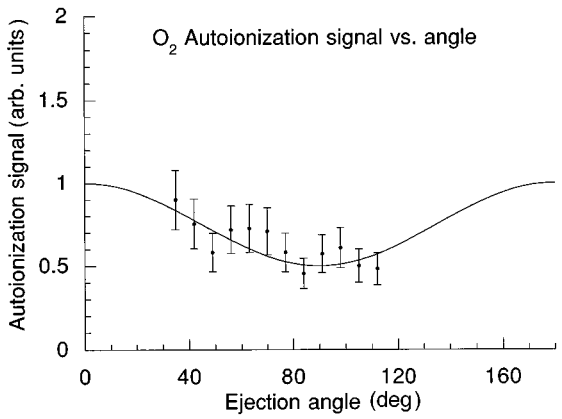

FIG. 3. Plot of response of the ejected electron analyzer to an isotropic flux of electrons produced by an autoionizing state of O_2 (Ref. [14]). The solid line is the function $0.5(1+\cos^2\theta_{ej})$.

single angle can be obtained in 10–20 min. This method measures the relative TDCS as a function of ejected electron angle directly whereas the spectrum mode measures all of the ionization processes at a fixed ejection angle. In principle, the relative TDCS as a function of ejected angle could be obtained in the spectrum mode by recording a complete coincidence energy-loss spectrum at each value of the ejected angle. However, since at least 12 h were required to complete a single spectrum, it was impossible to keep the incident current and other parameters from drifting significantly. The ''spectrum'' method was therefore of greatest use in determining the relative TDCS for the various ionization processes while the second ''ejected angle scan'' was most useful in determining the angular dependence of a single process as a function of θ_{ej}. The second method could only be used for the strong ionization signals from the $X\,^2\Sigma_g^+$ and $A\,^2\Pi_u$ states.

In order to determine the dependence of the TDCS on θ_{ej}, it is necessary to know the angular dependence of the scattering volume. Since the target gas source was a simple hypodermic needle, we expected that the interaction region consisting of the volume defined by the intersection of the angular acceptance cones of the three electron spectrometers might not be constant as θ_{ej} was varied. To investigate this point, we used the previously studied [15] autoionizing transition in O_2 near 16.8 eV to produce an isotropic flux of ejected electrons that could be detected in coincidence with the scattered electrons. Figure 3 shows an angular scan of the intensity of the autoionization coincidence peak with the accidental background removed. The intensity of the autoionization process as a function of θ_{ej} is well described by $(1+\cos^2\theta_{ej})$. This result is quite reasonable since it is between the typical $\cos\theta$ variation observed for static gas targets and the constant scattering volume obtained for a well-collimated molecular-beam target [1]. All the angular scans reported here were corrected by this factor.

As a test of the apparatus, we made measurements on argon and nitrogen for comparison with theory and previous results. Figure 4 shows a plot of the TDCS for 100-eV electrons on argon at a scattered electron angle of 4° and an ejected electron energy of 5 eV. Also included are the results of a distorted wave Born approximation calculation by Madison and Kravtsov [16] and experimental results by Ehrhardt *et al.* [17]. The present results have been normalized to the calculation at the peak of the binary lobe. Excellent agreement is obtained for the relative TDCS. The relative TDCS of the $3\sigma_g$ orbital of N_2 at 200 eV, 4°, and 10 eV was also measured. These results are compared to those of Avaldi *et al.* [7] at 270 eV, 3.5° and 10 eV in Fig. 5. Again, agreement within experimental error is obtained for the relative TDCS.

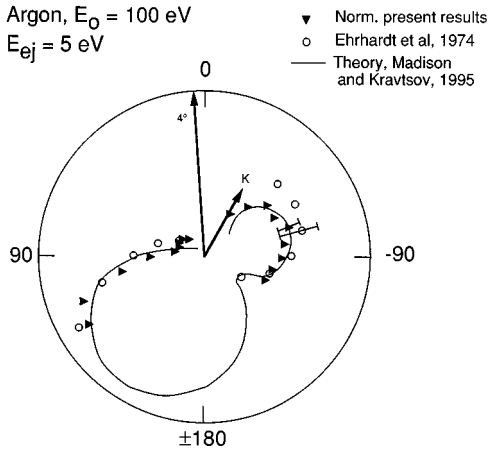

FIG. 4. Comparison of present relative 100-eV argon triple differential cross section to previous experimental work of Ehrhardt *et al.* (Ref. [17]) and theoretical calculation of Madison and Kravtsov (Ref. [16]). The present results have been normalized to the theoretical value at the maximum of the binary peak. The points representing the work of Ehrhardt *et al.* have been taken from the smooth curve presented by the authors.

RESULTS AND DISCUSSION

Plots of the relative TDCS as a function of θ_{ej} for ionization of the $3\sigma_g$ and $1\pi_u$ orbitals of N_2 are shown in Figs. 6 and 7. The data have been normalized to a common radial scale.

As mentioned before, first-order theories of ionization require that the binary and recoil lobes be symmetric about the

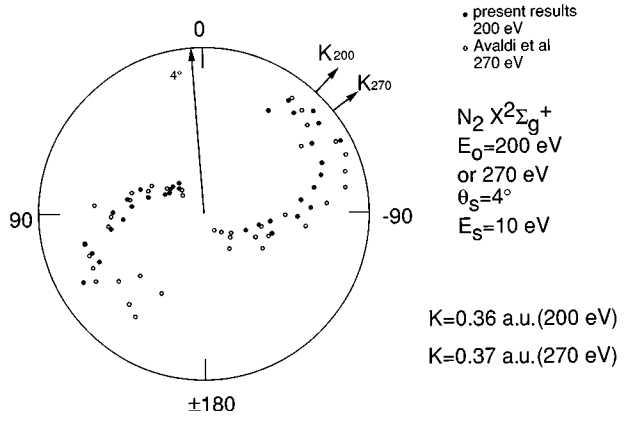

FIG. 5. Comparison of present 200-eV N_2 triple differential cross section to results of Avaldi *et al.* (Ref. [7]). The present relative results have been normalized to the results of Avaldi *et al.* at the maximum of the binary peak.

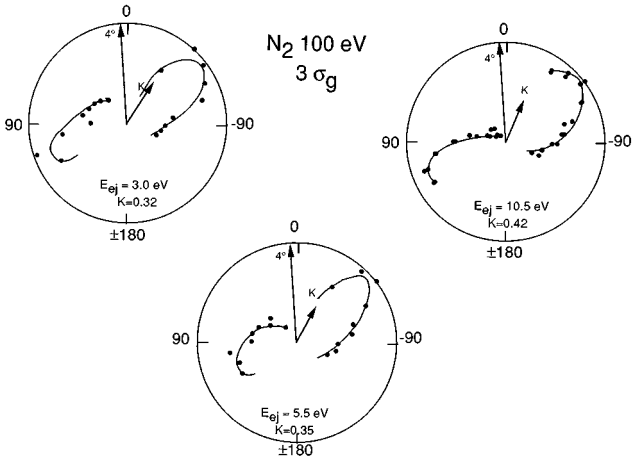

FIG. 6. Experimental results for N_2 triple differential cross section vs θ_{ej} for ionization of the $3\sigma_g$ orbital of N_2. The incident energy and scattered electron angle were 100 eV and 4° in all cases. Results are shown for E_{ej} of 3.0, 5.5, and 10.5 eV. The direction of the momentum transfer vectors is shown for each case as is the magnitude of the momentum transfer in atomic units. The points are the experimental data. The solid lines are fits to a three-point smoothed set of the experimental data points and are intended to guide the eye.

momentum transfer axis and the binary-recoil ratio approach unity as $K \rightarrow 0$ [1]. It is obvious from the data in Figs. 6 and 7 that there are large deviations from first-order behavior for N_2 at 100 eV. These deviations can be summarized as follows. (1) In all cases, the maximum of the binary lobe appears at a larger value of θ_{ej} than the momentum transfer direction θ_K. (2) In all cases, the maximum of the recoil lobe appears at a *smaller* value of θ_{ej} than the reverse **K** direction. (3) The maximum of the binary lobe for the $1\pi_u$ orbital ionization is at a much larger angle than that for the $3\sigma_g$ orbital (80° versus 50°). (4) The maxima of the recoil lobes are at approximately the same angle for all cases. (5) The symmetry axes of the two lobes do not coincide for the $3\sigma_g$ orbital. (6) The symmetry axes of the two lobes for the $1\pi_u$ orbital ionization approximately coincide. (7) The binary-recoil ratios in all cases are of the order of 1 ± 0.2.

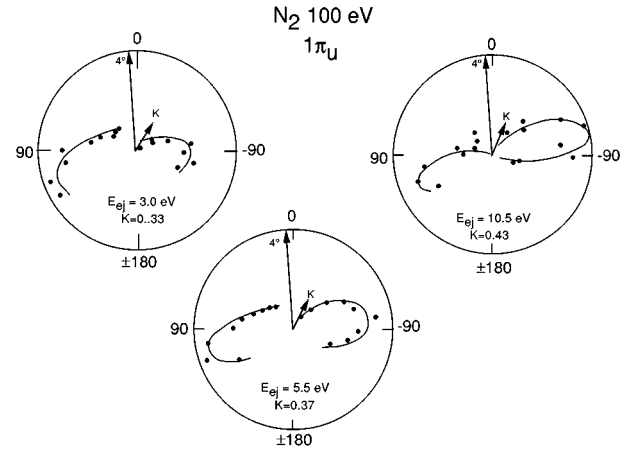

FIG. 7. Same as Fig. 6 except for ionization of the $1\pi_u$ orbital of N_2.

Feature (1) is unremarkable. It is typical of atomic systems [1]. On the other hand, the recoil peaks are displaced to smaller values of θ_{ej} than the reverse **K** direction. Displacement of the recoil maximum to smaller angles was first observed by Avaldi *et al.* [8] in their study of ionization of the $1s\ \sigma$ orbital of C_2H_2. The appearance of the same phenomenon in N_2 in clear contrast to the atomic case suggests that this may be a common feature in molecular ionization.

The large, 30°, difference in direction of the binary lobes for the two orbitals, noted as feature (3), is of great interest. As the present experiments appear to be the first in which the ionization of two different valence molecular orbitals in the same target can be compared, this phenomenon has not been previously reported. This feature, along with feature (2), the displacement of the maximum of the recoil lobes to smaller values of θ_{ej}, suggests that the interaction between the two outgoing electrons and the residual ion core is very different from what is found for atomic systems. The 50° maximum for the $3\sigma_g$ orbital binary peak is typical of atomic ionization. The fact that the maximum for the $1\pi_u$ orbital is at such a large angle may be evidence for a preferred orientation of the molecular axis with respect to the incident beam direction for ionization of this orbital.

The breaking of the common symmetry axis between the binary and recoil lobes is further evidence of higher-order interactions. For the $1\pi_u$ orbital, the apparent existence of a symmetry axis may be fortuitous, a consequence of the rotation of the binary lobe to larger angles.

The observed binary-recoil ratio of 1 ± 0.2 deserves comment in view of the very different results reported by Jung *et al.* [6] and the results of Avaldi *et al.* [7], which are very similar to ours. For $E_0 = 100$ eV, $\theta_0 = 8°$, and $E_{ej} = 3$ or 4 eV, the binary peak in the data of Jung *et al.* [6] resembles the present binary peak in shape. (Although nowhere stated, we assume that Jung *et al.* [6] were observing ionization of the $3\sigma_g$ orbital of N_2.) However, Jung *et al.* [6] report a very small recoil peak, with a binary-recoil ratio of 4.0 at $\theta_{ej} = 3$ eV, which changes to 100 at $\theta_{ej} = 4$ eV. In addition, the direction of the maximum of their binary lobe changes from 50° at 4 eV ($\theta_K = 47°$) to 65° ($\theta_K = 50°$) at 3 eV. It should be noted that the magnitude of K was the same (0.45 a.u.) for both 3- and 4-eV values of E_{ej}. Our data, for which the magnitude of K changes from 0.32 to 0.42, do not show such effects. The data of Avaldi *et al.* [7], although taken at a higher value of $E_0 = 270$ eV, have $K = 0.37$ and a binary-recoil ratio on the order of unity in agreement with our data. Nothing like the large changes in either binary-recoil ratio or direction of the binary maximum seen in the data of Jung *et al.* [6] appear in either the data of Avaldi *et al.* [7] or our data.

If the binary-recoil ratio were as large as Jung *et al.* [6] report, there should be an effect on the double differential ionization cross section. Very little intensity should be observed at angles greater than 90°. However, the measurements of Opal *et al.* [18] and Shyn [19], although they disagree at small angles and in the details of the cross section, show that the flux of electrons is almost isotropic at angles between 20° and 150°. It therefore appears that if these changes in the TDCS are real, they must occur over a very small range of the ionization parameters.

The most important variable in ionization processes is the

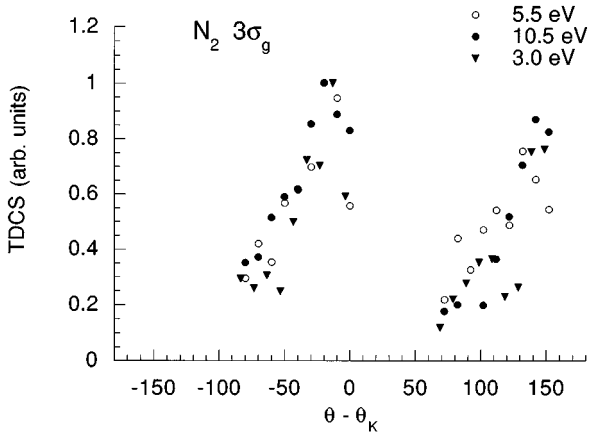

FIG. 8. Cartesian plot of TDCS for ionization of the $3\sigma_g$ orbital of N_2. The results for the three values of E_{ej} indicated are plotted vs the difference between θ_{ej} and the momentum transfer direction θ_K.

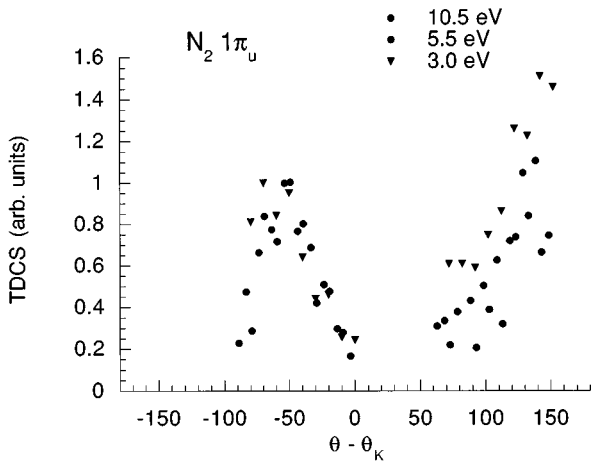

FIG. 9. Same as Fig. 8 except for the $1\pi_u$ orbital of N_2.

momentum transfer vector [1]. In the $3\sigma_g$ orbital ionization, for $E_{ej}=10.5$ eV, K varies from 0.38 a.u. at $\theta_0=0°$ to 0.58 a.u. at 10°. Correspondingly, at $E_{ej}=3.0$ eV, the variation is from 0.38 to 0.52 a.u. θ_K varies from 0 to 55° over the same range at 3.0 eV and 0 to 44° at 10.5 eV. This small variation in the magnitude of K suggests that the shapes of the observed distributions should be the same for different values of E_{ej}. Figures 8 and 9 show the TDCS data for the two orbitals plotted as a function of the angle measured from θ_K. Although there are some small differences, it is obvious that the distributions can be roughly superimposed. This also suggests that in view of the rather small changes in K out to $\theta_0=10°$, our 4° data should be representative of the whole region.

CONCLUSIONS

An $(e,2e)$ experiment has been performed in which ionization of two molecular orbitals in the same target can be compared at an incident energy corresponding to the peak of the total ionization cross section and momentum transfer in the intermediate region. Large deviations from the predictions of first-order theory are observed. Although the ionization potentials of the $3\sigma_g$ and $1\pi_u$ orbitals are only 1.11 eV apart, there are marked differences in the TDCS for ionization of the two orbitals. These differences are evidence for the sensitivity of the $(e,2e)$ experiments of the present type to differences in the interaction of the incident electron with the wave functions of the two orbitals in initial state as well as differences in the interaction of the two outgoing electrons with the residual ion cores.

The observed deviations from first-order theory predictions are in some cases opposite to those observed in atomic systems. Particularly interesting is the change in the direction of the recoil lobe maximum towards smaller angles observed in both these experiments and those of Avaldi *et al.* [7]. Ejection of an electron in the recoil direction requires a stronger interaction between the ejected electron and the ion core than ejection in the binary direction. This effect may be an extremely sensitive probe of the ion charge density and other quantities.

The sensitivity to initial and final-state properties of the target makes experiments such as the present ones a powerful tool for investigating ion states. However, the theory of $(e,2e)$ processes in the low incident energy, medium momentum transfer region is difficult [1] and advances in theory will be required before these effects can be understood in detail.

ACKNOWLEDGMENTS

This work was supported by Grant No. ATM-9222344. The authors also thank M. A. Coplan and J. H. Moore for many valuable discussions.

[1] H. Ehrhardt, K. Jung, G. Knoth, and P. Schlemmer, Z. Phys. D **1**, 3 (1986).
[2] A. Lahmam-Bennani, J. Phys. B **24**, 2401 (1991).
[3] M. Coplan, J. Moore, and J. Doering, Rev. Mod. Phys. **66**, 985 (1994).
[4] M. J. Van der Wiel and C. E. Brion, J. Electron. Spectrosc. Relat. Phenom. **1**, 309 (1973); **1**, 443 (1973).
[5] M. Cherid, A. Lahmam-Bennani, A. Duguet, R. Zurales, R. Lucchese, M. Dal Capello, and C. Dal Capello, J. Phys. B **22**, 3483 (1989).
[6] K. Jung, E. Schubert, D. A. L. Paul, and H. Ehrhardt, J. Phys. B **8**, 1330 (1975).
[7] L. Avaldi, R. Camilloni, E. Fainelli, and G. Stefani, J. Phys. B **25**, 3551 (1992).
[8] L. Avaldi, R. Camilloni, and G. Stefani, Phys. Rev. A **41**, 134 (1990).
[9] E. Krishnakumar and S. K. Srivastava, J. Phys. B **23**, 1893 (1990).
[10] J. Doering and L. Goembel, J. Geophys. Res. **96**, 16 025 (1991).

[11] L. Goembel, J. Yang, and J. Doering, J. Geophys. Res. **99**, 17 477 (1994).
[12] J. Doering, E. Gulcicek, and S. Vaughan, Chem. Phys. Lett. **114**, 334 (1985).
[13] L. Goembel and J. Doering, Rev. Sci. Instrum. **66**, 3472 (1995).
[14] J. Doering, J. Yang, and J. W. Cooper, Chem. Phys. Lett. **232**, 159 (1995).
[15] D. Dahl and J. Delmore, Idaho National Engineering Laboratory, Informal Report No. EGG-CS-7233, Rev. 2 1988 (unpublished).
[16] D. Madison and V. D. Kravtsov (private communication) [theory described in T. Roesel, J. Roeder, L. Frost, K. Jung, H. Ehrhardt, S. Jones, and D. H. Madison, Phys. Rev. A **46**, 2539 (1992)].
[17] H. Ehrhardt, K. Hesselbacher, K. Jung, E. Schubert, and K. Williams, J. Phys. B **7**, 69 (1974).
[18] C. Opal, C. Beaty, and W. K. Peterson, At. Data **4**, 209 (1972).
[19] T. W. Shyn, Phys. Rev. A **27**, 2383 (1987).